

UC Irvine

UC Irvine Previously Published Works

Title

Isotopic signature of extreme precipitation events in the western U.S. and associated phases of Arctic and tropical climate modes

Permalink

<https://escholarship.org/uc/item/3pr746jk>

Journal

Journal of Geophysical Research: Atmospheres, 121(15)

ISSN

2169-897X

Authors

McCabe-Glynn, Staryl
Johnson, Kathleen R
Strong, Courtenay
[et al.](#)

Publication Date

2016-08-16

DOI

10.1002/2016jd025524

Peer reviewed

RESEARCH ARTICLE

10.1002/2016JD025524

Key Points:

- 90% of the extreme precipitation events at California site occurred during the negative Arctic Oscillation
- Extreme events show diverse isotopic signatures, but composite resembles full study period mean
- Strongest precipitation anomalies occur when negative AO, negative PNA, and positive SOI are in sync

Supporting Information:

- Supporting Information S1

Correspondence to:

S. McCabe-Glynn,
mccabegs@uci.edu

Citation:

McCabe-Glynn, S., K. R. Johnson, C. Strong, Y. Zou, J. Y. Yu, S. Sellars, and J. M. Welker (2016), Isotopic signature of extreme precipitation events in the western U.S. and associated phases of Arctic and tropical climate modes, *J. Geophys. Res. Atmos.*, *121*, 8913–8924, doi:10.1002/2016JD025524.

Received 28 JUN 2016

Accepted 8 JUL 2016

Accepted article online 26 JUL 2016

Published online 12 AUG 2016

Isotopic signature of extreme precipitation events in the western U.S. and associated phases of Arctic and tropical climate modes

Staryl McCabe-Glynn¹, Kathleen R. Johnson¹, Courtenay Strong², Yuhao Zou³, Jin-Yi Yu¹, Scott Sellars⁴, and Jeffrey M. Welker⁵

¹Department of Earth System Science, University of California, Irvine, California, USA, ²Department of Atmospheric Sciences, University of Utah, Salt Lake City, Utah, USA, ³Discover Financial Services, Riverwoods, Illinois, ⁴Center for Western Weather and Water Extremes, Scripps Institution of Oceanography, University of California, San Diego, California, USA, ⁵Department of Biological Sciences, University of Alaska Anchorage, Anchorage, Alaska, USA

Abstract Extreme precipitation events, commonly associated with “Atmospheric Rivers,” are projected to increase in frequency and severity in western North America; however, the intensity and landfall position are difficult to forecast accurately. As the isotopic signature of precipitation has been widely utilized as a tracer of the hydrologic cycle and could potentially provide information about key physical processes, we utilize both climate and precipitation isotope data to investigate these events in California from 2001 to 2011. Although individual events have extreme isotopic signatures linked to associated circulation anomalies, the composite across all events unexpectedly resembles the weighted mean for the entire study period, reflecting diverse moisture trajectories and associated teleconnection phases. We document that 90% of events reaching this location occurred during the negative Arctic Oscillation, suggesting a possible link with higher-latitude warming. We also utilize precipitation data of extreme precipitation events across the entire western U.S. to investigate the relationships between key tropical and Arctic climate modes known to influence precipitation in this region. Results indicate that the wettest conditions occur when the negative Arctic Oscillation, negative Pacific/North American pattern, and positive Southern Oscillation are in sync and that precipitation has increased in the southwestern U.S. and decreased in the northwestern U.S. relative to this phase combination’s 1979–2011 climatology. Furthermore, the type of El Niño–Southern Oscillation event, Central Pacific or Eastern Pacific, influences the occurrence, landfall location, and isotopic composition of precipitation.

1. Introduction

Extreme precipitation events can contribute extensively to replenishing reservoirs and groundwater supplies, though simultaneously, can result in harmful consequences for the U.S. West Coast, including excessive snowfall, flooding, landslides, property damage, and loss of life [Dettinger, 2011; Mass et al., 2011]. One of the most prevalent extreme precipitation events that occur along the west coast of North America are “Atmospheric Rivers” (AR), elongated pathways of extensive atmospheric moisture transport over the ocean which can lead to substantial precipitation and flooding when they make landfall [Ralph and Dettinger, 2011; Ralph et al., 2013]. California’s largest and most severe storms and essentially all major historical floods have been associated with landfalling ARs [Dettinger, 2011]. For example, a strong AR that occurred 17 to 22 December 2010 produced up to 670 mm of precipitation in Southern California [Ralph and Dettinger, 2012] and exceptional snowfall in California’s Sierra Nevada Mountains [Guan et al., 2013]. Another AR in early January 2005 produced more than 1016 mm of rainfall in Southern California in only 4 days, causing widespread flooding and a massive mudslide resulting in 10 fatalities. Given that water supply and flood risks in California are strongly linked with AR occurrence and the intensity and landfall position are difficult to forecast accurately [Wick et al., 2013], improved short-term forecasts and seasonal model projections of ARs are needed for better planning and mitigation efforts.

Extreme precipitation events are projected by most global climate models to become more prevalent as the climate changes [Dettinger, 2011; Hagos et al., 2016], largely due to increased water vapor content in a warmer atmosphere [Trenberth, 1999]. Multiple climate models project more years with many AR episodes and higher-than-historical water vapor transport rates, indicating that California flood risks may increase beyond those previously known [e.g., Dettinger, 2011; Lavers et al., 2015]. Airborne and ship-borne facilities, modern

satellite advances, land-based sensors, and modeling studies have led to enhanced understanding of characteristics and mechanisms leading to extreme precipitation events. For example, recent field campaigns such as the CalWater study suggest that large-scale atmospheric circulation can transport aerosols from Asia across the Pacific, thereby increasing the amount of cloud condensation nuclei that can form into cloud droplets, playing an important role in landfalling ARs in California [Ault *et al.*, 2011; Creamean *et al.*, 2013]. There is still significant uncertainty surrounding the water vapor budget of ARs, however, in part due to the inability of satellite observations to record winds at the altitude of maximum water vapor flux [Ralph *et al.*, 2015]. Significant uncertainty also still exists for short-term seasonal projections, despite recent efforts to identify predictive climate relationships (e.g., statistical relationships between coupled climate modes and AR occurrence). Several sources of uncertainty currently limit AR predictability, including limited spatial resolution, lack of process understanding, the short observational record, and the large magnitude of internal variability [e.g., Dettinger, 2011].

The stable isotope composition of precipitation ($\delta^{18}\text{O}$ and δD) is widely utilized as a tracer of the hydrologic cycle in general circulation models, in modern observations, and as recorded in natural archives of past climate, such as ice cores, tree ring cellulose, and speleothems [e.g., Berkelhammer and Stott, 2008; Yoshimura *et al.*, 2008; McCabe-Glynn *et al.*, 2013], yet isotopes have not been extensively investigated in AR precipitation. The climatic controls on precipitation isotopes are complex and numerous and include temperature, rainfall amount, relative humidity, moisture recycling, condensation height, and moisture source region [e.g., Gat, 1996; Buening *et al.*, 2012]. Robust interpretation of precipitation isotope variability requires a strong understanding of the climatic controls on the isotopic composition of modern precipitation on a range of spatial and temporal scales [Liu *et al.*, 2014]. Isotopes of water undergo temperature-dependent fractionation during evaporation and condensation as water molecules move throughout the hydrologic cycle. Essentially, the water molecules composed of the light isotopes (^{16}O and ^1H) are preferentially evaporated, whereas those with one or more heavy isotopes (^{18}O and ^2H) are preferentially condensed and the magnitude of these effects depends on temperature [Craig, 1961]. This leads to predictable spatial and temporal variability in the isotopic composition of precipitation, which correlates with climatic and geographic factors such as condensation temperature, rainfall amount, relative humidity, moisture source region, latitude, altitude, and distance from coast [Dansgaard, 1964; Gat, 1996]. Detailed water isotope data from AR events impacting the western U.S. may be helpful for constraining the water budget of these events, which is still an important question in AR research. For instance, precipitation isotopes may be used to assess the fraction of water that is directly sourced from distal locations versus continually added through horizontal advection along the AR trajectory [Yoshimura *et al.*, 2010]. Furthermore, if ARs are shown to have a unique isotopic signature, then this could enable the development of extended records of AR frequency and/or magnitude utilizing precipitation $\delta^{18}\text{O}$ variations preserved in paleoclimate archives such as tree ring cellulose and speleothem $\delta^{18}\text{O}$.

Coupled ocean-atmosphere modes in the Pacific, such as the El Niño–Southern Oscillation (ENSO) and the Pacific Decadal Oscillation (PDO), and atmospheric pressure patterns, such as the Arctic Oscillation (AO) and Pacific/North American (PNA) pattern, are known to exert substantial control on the hydroclimate of western North America through their combined influence on midlatitude storm trajectories [e.g., Cook *et al.*, 2007; MacDonald and Case, 2005; Rodionov *et al.*, 2007; Wise and Dannenberg, 2014]. Prior research indicates the isotopic composition of precipitation in California is largely determined by the moisture source region and storm tracks delivering precipitation to this region, indicating that stable isotopes might serve as a useful tracer of past changes in synoptic-scale climate patterns [Friedman *et al.*, 1992; Berkelhammer *et al.*, 2012]. For example, $\delta^{18}\text{O}$ during El Niño events has recently been shown to be depleted by 2–3‰ in California relative to the long-term mean [Welker, 2012], potentially reflecting a greater contribution of moisture from the North Pacific. Given that ARs can contribute up to 50% of the water year precipitation in the western U.S. [Dettinger, 2011], an improved understanding of the isotopic signals associated with AR precipitation is critical for numerous water isotope applications, in addition to improving understanding of AR dynamics and history.

Increased contribution of ARs to annual precipitation totals has been associated with positive ENSO and PDO for some parts of the western U.S., especially in Southern California, but the complex interplay of multiple climate factors thus far limits the utility of these relationships for short-term prediction [Cayan *et al.*, 2016]. Dettinger [2011] found that average AR (specifically the Pineapple Express-type) contribution to water year precipitation in Central and Northern California is correlated with November–April sea surface temperatures

(SSTs) in the northwestern Pacific Ocean, just north of the Kuroshio Extension region. Furthermore, a recent paleoclimate study indicates that the isotopic composition of precipitation ($\delta^{18}\text{O}$) as recorded in a stalagmite from the southern Sierra Nevada mountains is also linked to SSTs in the Kuroshio Extension region [McCabe-Glynn *et al.*, 2013], including in the location shown to influence AR precipitation [Dettinger, 2011]. This relationship is likely manifested through the influence of SST patterns on the trajectory of storms reaching the western U.S., as anomalously high SSTs can provide heat fluxes that generate an atmospheric wave, shifting the jet stream north over the western Pacific and south over the eastern Pacific [Ren *et al.*, 2008] and therefore suggests a possible link between ARs and annual mean precipitation isotopes. A recent study found that the majority of AR events (86%) over the West Coast of the U.S. are grouped into three trajectory types [Ryoo *et al.*, 2015] from variable origins; thus, these events likely carry unique water isotope properties that could potentially be utilized to provide information about moisture source region, water vapor budgets, and other key physical processes of AR events [Vachon *et al.*, 2010].

In this paper, we present weekly precipitation amount and isotopic data from a site in Southern California that was affected by 22 extreme precipitation events (defined as >100 mm/week) between 2001 and 2011. We investigate the relationship between the oxygen isotope composition of these events and a range of climate factors to better constrain AR processes. Additionally, we utilize the North American Regional Reanalysis (NARR) precipitation data to investigate the relationships between extreme precipitation events in the entire western U.S. and key climate modes known to influence precipitation in this region. The results presented here will contribute to improved process understanding of AR events and potentially lead to more robust short-term and seasonal projections of extreme precipitation in the western U.S. The results will also lead to better understanding of the impact of ARs and related climate modes on mean annual precipitation isotopes in this region and thus contribute to improved interpretation of oxygen-isotope-based paleoclimate records from California [e.g., McCabe-Glynn *et al.*, 2013].

2. Analysis and Results

2.1. Study Site and Precipitation Samples

We conducted 220 stable isotope analyses of weekly precipitation samples collected by the National Atmospheric Deposition Program from 2001 to 2011 at Giant Forest in Sequoia National Park, California (CA-75; 36.57°N, 118.78°W; 1921 m) (Figure 1 (black star) and Table S1 in the supporting information) [Berkelhammer *et al.*, 2012]. See supporting information for details of sample collection and analysis. This site is ideally located on the southwestern flank of the Sierra Nevada Mountains which receives the majority of precipitation during the winter from Pacific storm tracks. We found an average water year (October to September) precipitation amount of 977 ± 387 mm with an average amount weighted $\delta^{18}\text{O}$ of $-12.11 \pm 1.18\text{‰}$ and δD of $-81.6 \pm 8.9\text{‰}$ (Table S4). Of the 220 samples, we chose to focus on the top 10 (>150 mm) and top 22 (10%; >100 mm) weeks with the highest precipitation amounts. We identified which of these high-precipitation weeks were impacted by landfalling AR events utilizing previously developed methods for AR identification [Zhu and Newell, 1998; Ralph *et al.*, 2004; Neiman *et al.*, 2008]. Results show that 9 of the top 10 and 16 of the top 22 weeks contain AR events [Neiman *et al.*, 2008] (Table S2).

Isotopic analyses of precipitation that fell during the 22 wettest weeks show large variability ($\delta^{18}\text{O}$ range of -7.20‰ to -19.27‰ ; δD range of -49.5 to -150.0‰ ; d -excess range of 4.1 to 25.8; Table S2), reflecting the complex influences on the isotopic composition of precipitation in California [e.g., Berkelhammer *et al.*, 2012; Friedman *et al.*, 1992; Buening *et al.*, 2012]. As there is no single isotopic signature associated with AR events, the potential for reconstructing them from the isotopic paleoclimate data does not appear to be very promising. Linear regression analysis shows no significant $\delta^{18}\text{O}$ relationship with P and only a weak positive correlation with surface T ($r^2 = 0.13$, $p = 0.0936$). A multiple linear regression of $\delta^{18}\text{O}$ as a function of both surface T and P indicates that these factors combined could explain up to 25% of the variance in $\delta^{18}\text{O}$ for the top 22 precipitation weeks. The remaining variability must be explained by other factors. Results of back trajectory analyses conducted for the top 10 precipitation weeks utilizing Hysplit show a wide range of storm trajectories, and hence moisture source regions, which could have contributed to the highly variable $\delta^{18}\text{O}$ and d -excess values (supporting information Figure S1). To investigate this further, we conducted detailed analysis of climatic characteristics of these events and also examined the influence of key climate modes which are known to influence the trajectory of storms reaching the western U.S.

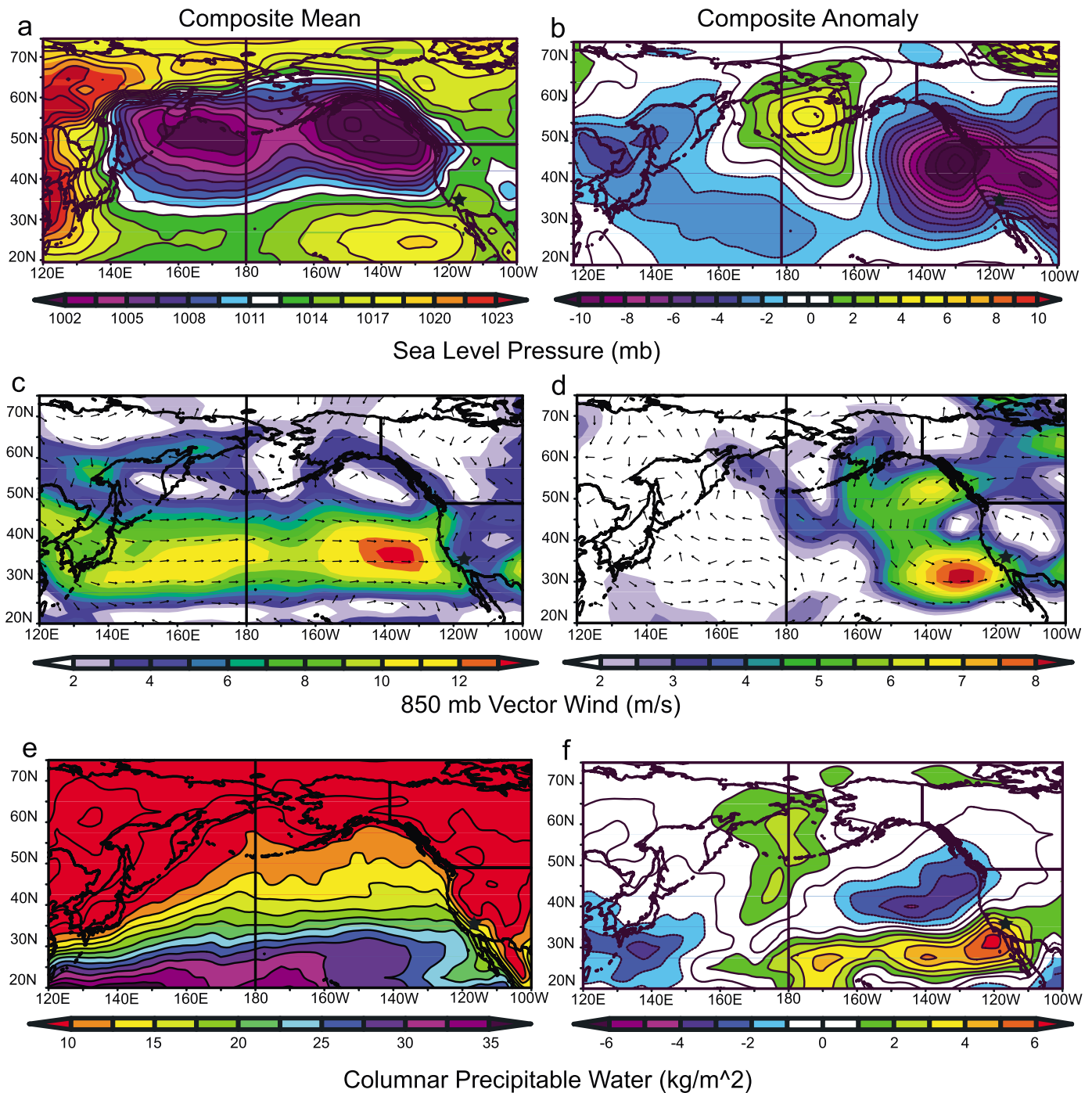


Figure 1. Composite analysis maps during extreme precipitation events show mean and anomaly maps derived from the NCAR daily reanalysis data set for all precipitation events during the top 10 weeks (>150 mm) (Table S2): (a and b) sea level pressure (mbar); (c and d) 850 mbar winds (m/s); and (e and f) columnar precipitable water (kg/m^2) (anomaly from the mean of 1981–2010 climatology). Black star shows study location site Giant Forest in Sequoia National Park, California. Image produced utilizing the plotting tools provided by the NOAA/ESRL Physical Sciences Division, Boulder, Colorado, on their website at <http://www.esrl.noaa.gov/psd/>.

2.2. Climatic Conditions During Extreme Precipitation Events

We utilized National Center for Atmospheric Research/National Centers for Environmental Prediction (NCAR/NCEP) reanalysis data to construct composite mean and anomaly maps of sea level pressure (SLP), 850 mbar vector winds, and columnar precipitable water for all days with measurable precipitation during the 10 wettest weeks at our site (supporting information Table S5). Results show the dominant mean sea level

pressure (SLP) pattern is a weakened and split Aleutian Low (Figure 1a). The deep offshore trough located northwest of California (Figure 1b) coupled with anomalously cyclonic 850 mbar winds (Figures 1c and 1d) and enhanced subtropical columnar precipitable water (Figures 1e and 1f) lead to heavy rainfall in the southwestern U.S. (Figures S2a and S2b). The composite SLP patterns are similar to those observed during La Niña-like conditions [Rodionov *et al.*, 2007] which are associated with a weaker and strongly meridional jet stream, with a greater north-south orientation. Similar SLP anomalies are observed during the negative phase of the Arctic Oscillation (AO) [Francis and Vavrus, 2012] and the negative phase of the Pacific/North American (PNA) pattern, suggesting that these may also play a role.

In either case, this amplified wave structure is conducive to midlatitude cyclones traveling equatorward, obtaining moisture over the tropical Pacific, and directing it toward the study site (Figure 1d). Precipitation during these events would be expected to be enriched in ^{18}O due to increased contribution of subtropical moisture [e.g., McCabe-Glynn *et al.*, 2013]; however, the weighted mean $\delta^{18}\text{O}$ observed during the top 10 events ($-12.82 \pm 3.78\text{‰}$) is similar to the weighted mean for the entire study period (2001–2011) suggesting either that the moisture source signal may be obscured by other factors and/or that moisture is added along the entire trajectory through horizontal advection as others have suggested [e.g., Yoshimura *et al.*, 2010].

2.3. Climate Mode Influence on Extreme Precipitation

2.3.1. Arctic Oscillation and Pacific/North American Pattern

To further investigate these large precipitation events, we compared them with key climate indices known to influence precipitation in the western U.S. (Table S2; we define positive values as ≥ 0.5 , neutral values between -0.5 and 0.5 , and negative values as ≤ -0.5). The Arctic Oscillation (AO) is a large-scale climate mode associated with varying sea level pressure patterns poleward of 20°N , which are known to exert a strong influence on weather in North America. It is worth noting that 90% of the top 10 precipitation weeks (73% of the top 22 precipitation weeks) coincided with the negative phase of the AO ($p < 0.0001$), consistent with findings of an earlier study [Guan *et al.*, 2013]. The negative AO is characterized by high-pressure anomalies in the Arctic and low-pressure anomalies in the surrounding lower latitudes, which leads to weaker westerlies in the upper atmosphere [Thompson and Wallace, 2000].

To explore the dynamic links between ARs and the Arctic Oscillation, we utilized a unique satellite-based precipitation data set, Precipitation Estimation from Remotely Sensed Information using Artificial Neural Networks (PERSIANN), to investigate the spatiotemporal characteristics of extreme precipitation events to investigate the spatiotemporal characteristics of extreme precipitation events during the top 22 precipitation weeks at our site [Sellars *et al.*, 2013]. Precipitation events were identified by applying an object-based connectivity algorithm (PERSIANN-CONNECT) to organize the remotely sensed precipitation data in to discrete precipitation events or “objects.” Utilizing a minimum threshold of 1 mm/h for 24 h, we identified individual storm events that occurred during 17 of the top 22 precipitation weeks at our site. A descriptive statistics algorithm was utilized to calculate physical characteristics of each storm event (Table S3), including event speed, maximum precipitation intensity, and duration [Sellars *et al.*, 2013]. We find that the highest volume events that hit California during the negative AO are characterized by slower average speeds (44 ± 12 km/h), increased maximum precipitation intensity (26 ± 13 mm/h), and longer duration (104 ± 68 h) than those that occur during the positive AO (speed: 55 ± 17 km/h; maximum precipitation intensity: 19 ± 9 mm/h; duration: 78 ± 59 h). Additionally, the starting latitude of the object during the negative AO was higher ($37.78^\circ\text{N} \pm 5.64$) and had a more westerly starting longitude ($186.12^\circ\text{W} \pm 38.15$) than during the positive AO ($30.66^\circ\text{N} \pm 3.57$; $197.79^\circ\text{W} \pm 42.26$). These results suggest that AR events that occur when the AO is negative tend to have greater and more intense precipitation and are therefore likely associated with increased flood risk.

While the AO can vary considerably on short timescales and the causes of variability are not entirely known, Strong and Magnusdottir [2008] showed that the AO arises from a positive feedback associated with tropospheric Rossby wave breaking, which has also been previously linked to AR events [Payne and Magnusdottir, 2014]. Recent studies link shifts in the jet stream and increased persistence of midlatitude weather patterns to apparent decreases in the AO during winters preceded by reduced summer Arctic sea ice [e.g., Francis and Vavrus, 2012]. Arctic amplification may therefore increase the likelihood of extreme precipitation events in the western U.S. through its influence on the AO and the jet stream. However, additional research on the link between the AO, ARs, and high-latitude warming is needed to fully assess this potential mechanism, especially given that the manifestation of the AO over the Pacific sector is relatively

weak [Deser *et al.*, 2000] and the idea that meridional flow arises from Arctic amplification is controversial [Barnes, 2013; Screen and Simmonds, 2014].

The Pacific/North American (PNA) pattern is another prominent mode of variability in the extratropical Northern Hemisphere atmosphere. Similar to the AO, the PNA is closely associated with the Aleutian Low and related variations in the strength and position of the jet stream that exert a strong influence on regional climate in North America [Overland *et al.*, 1999]. During the positive PNA phase, enhanced pressure differences between the high-pressure ridge over the Rocky Mountains and the low-pressure trough over the southeastern U.S. leads to an enhanced meridional flow. Conversely, the negative PNA phase is associated with weaker pressure differences and a more zonal jet across North America. Due to this strong association between the PNA, the AO, and the jet stream, it is also possible that this mode influences the occurrence of extreme precipitation events in the western U.S. Investigation of the PNA index during the 22 wettest weeks of our study period show that extreme precipitation occurred similarly between the positive (7 weeks), negative (6 weeks), and neutral PNA phase (9 weeks) (Table S2). These results differ from previous findings which report increased AR frequency during the negative PNA [Guan *et al.*, 2013], though this effect is shown to be strongest when the negative AO occurs together with the negative PNA. Furthermore, the PNA pattern is influenced by the El Niño–Southern Oscillation (ENSO), so that the positive phase of the PNA pattern tends to be associated with El Niño conditions and the negative phase tends to be associated with La Niña conditions. Guan *et al.* [2013] also found enhanced AR snow accumulation in the Sierra Nevada during particularly cold events associated with negative AO, negative PNA, and La Niña conditions, indicating that this combination in particular should lead to enhanced extreme precipitation in California.

2.3.2. El Niño–Southern Oscillation

ENSO is also known to exert strong control on southwestern U.S. hydroclimate through modulation of the Pacific westerly jet and associated storm tracks. Numerous studies have shown that winter precipitation in the southwestern U.S. increases during El Niño events and decreases during La Niña events. Extreme precipitation events may also be strongly influenced by atmospheric variability associated with ENSO. We conducted an analysis of various ENSO-related indices during the top 22 precipitation weeks to assess the impact of ENSO on extreme precipitation at our site (Table S2). Analysis of the Oceanic Niño Index (ONI), based on sea surface temperature (SST) in the east central tropical Pacific Ocean, in which warmer SSTs indicate El Niño conditions and cooler, La Niña, indicates that 8 of the weeks fell during El Niño years, 8 fell during La Niña years, and 6 fell during neutral years, suggesting no significant relationship with SST-based indices. However, investigation of the daily Southern Oscillation Index, which is based on the difference between the atmospheric sea level pressure at Tahiti and at Darwin, showed that extreme precipitation events occurred more frequently during the positive SOI (10 weeks) and neutral SOI (10 weeks) than during the negative SOI (2 weeks). Similarly, when the monthly SOI was examined, extreme events occurred dominantly during the positive SOI (12 weeks) as opposed to the negative (6 weeks) and neutral (4 weeks) SOI. We also investigated the SOI phases [Stone *et al.*, 1996] and found that only 2 of the weeks occurred during SOI phase 1, defined as “consistently negative” (El Niño), whereas 11 weeks fell during SOI phase 2, defined as “consistently positive” (La Niña) conditions. Together, these results indicate that extreme precipitation occurs more frequently at our study site when the SOI is positive, which is often associated with La Niña conditions. However, this pattern appears when using the daily and the monthly SOI, but use of SST-based indices such as the ONI does not yield similar results. This possibly reflects influence of short-term weather-related atmospheric disturbances on AR occurrence, such as those related to the Madden-Julian Oscillation or other more transient events, which affect the SOI but not the tropical Pacific SST patterns.

To further assess the link between tropical Pacific SSTs and extreme precipitation events, we investigated whether the specific SST anomaly patterns associated with different ENSO types [Kao and Yu, 2009; Yu and Kao, 2007], Central Pacific (CP) versus Eastern Pacific (EP), influenced extreme precipitation event occurrence, location, and isotopic composition at our site. The two different types of El Niño are distinguished by different spatial locations of sea surface temperature anomalies in the tropical Pacific. The CP type (Figure S3b) is characterized by SST anomalies that are confined around the International Date Line, whereas the EP type (Figure S3c) has the more canonical SST pattern, with the largest anomalies located off the South American coast [Yu *et al.*, 2012; Zou *et al.*, 2014]. While the conventional EP ENSO results from the interaction with the Walker circulation and the CP ENSO results from the interaction between the tropical Pacific Ocean

and the Hadley circulation, both types have a distinct extratropical teleconnection pattern [Yu *et al.*, 2012] and thus may be expected to influence extreme precipitation events in western North America differently.

Investigation of the EOF-based CP and EP indices [Kao and Yu, 2009; Yu and Kim, 2010] during the top 22 precipitation weeks at our site show that extreme precipitation events occurred most frequently during the EP neutral (11 weeks) and negative modes (8 weeks), and only rarely during the EP positive mode (3 weeks). However, extreme precipitation events occurred about equally during both the negative (11 weeks) and positive (8 weeks) CP modes and were rare during the neutral phase (3 weeks) (Table S2). These results indicate that the type of ENSO event may influence the likelihood of extreme precipitation events affecting Southern California, with extreme precipitation events being more likely during a CP El Niño event than during an EP one. This different extreme precipitation response to the type of El Niño may reflect the stronger northward displacement of the subtropical jet during CP El Niño events than during EP ones, which is more conducive to delivery of precipitation to our site in Southern California. However, during the study period, 3 years were classified as CP-type El Niño years, while only 1 year was classified as an EP El Niño year [Yu *et al.*, 2012], so the relationship between ENSO type and AR frequency is tentative and needs further study.

Analysis of stable isotope signals during the various ENSO phases reveals that the mean $\delta^{18}\text{O}$ of extreme precipitation that fell during El Niño events, as defined by the ONI, is more positive ($-10.59 \pm 2.31\text{‰}$) than during La Niña events ($-13.28 \pm 3.55\text{‰}$), suggesting that extreme precipitation during El Niño events may contain a greater fraction of moisture derived from the tropical and subtropical Pacific compared with those during La Niña events. This is opposite to the ENSO- $\delta^{18}\text{O}$ relationship observed in other studies of mean annual precipitation $\delta^{18}\text{O}$, which have suggested that El Niño years are characterized by more negative $\delta^{18}\text{O}$ values overall [e.g., Welker, 2012]. If we assume that both observations are accurate, the increased $\delta^{18}\text{O}$ of AR precipitation during El Niño events at the same time as more negative annual mean precipitation $\delta^{18}\text{O}$ could potentially be explained by a simple mass balance model. If total weighted annual mean $\delta^{18}\text{O}$ is a function of isotopically enriched AR precipitation and isotopically depleted North Pacific sourced precipitation, the depleted North Pacific signal could be large enough to swamp the positive signals from AR precipitation in the annual mean values. We might expect more depleted precipitation overall during El Niño due to greater access to North Pacific moisture sources when the jet stream is situated farther to the south. Furthermore, however, we would need to explain why ARs during El Niño events overall are more positive than during La Niña events. This could potentially be explained by cooler temperatures, increased snowfall, and/or increased precipitation intensity during La Niña AR events. Guan *et al.* [2013] found that increased snow accumulation in the Sierra Nevada Mountains during the negative AO, PNA, and La Niña but that ARs are stronger during El Niño than La Niña conditions from 1998 to 2011. More consistent with our findings though, other studies have shown that ARs/extreme precipitation events along the west coast of North America are most pronounced during neutral/near-neutral ENSO conditions [Dettinger, 2004] or during La Niña years [Feldl and Roe, 2011].

2.4. Extreme Precipitation in the Western U.S. During Climate Mode Combinations

To investigate the dynamics of how large-scale climate modes interact to influence atmospheric circulation patterns and extreme precipitation across the western U.S., we combined pertinent climate indices (AO, PNA, SOI, EP, CP, PDO, and North Pacific Index) known to influence atmospheric circulation patterns delivering precipitation to the western U.S. with daily extreme precipitation events from 2001 to 2011 (Figures S3a–S3e). We created composite maps of anomalous precipitation (mm) during different climate mode combinations utilizing the NCEP North American Regional Reanalysis (NARR), a high-resolution regional-scale data set (Figures 2 and S3a–S3e). NARR precipitation has previously been shown to be superior to other reanalysis products [Bukovsky and Karoly, 2007], reflecting the fact that detailed precipitation observations were assimilated during the reanalysis process rather than fully parameterized [Mesinger *et al.*, 2006] such as in other products. Furthermore, the NARR has been shown to capture the intense precipitation rates and spatial patterns of precipitation during extreme events reasonably well, even over regions with complex topography, such as the western U.S. [Bukovsky and Karoly, 2007]. A main weakness of NARR precipitation is some disagreement with observations over the oceans and over parts of Canada where observational data are sparse, but as our study focuses on precipitation over land in the western U.S., this should not significantly impact our results [Mesinger *et al.*, 2006].

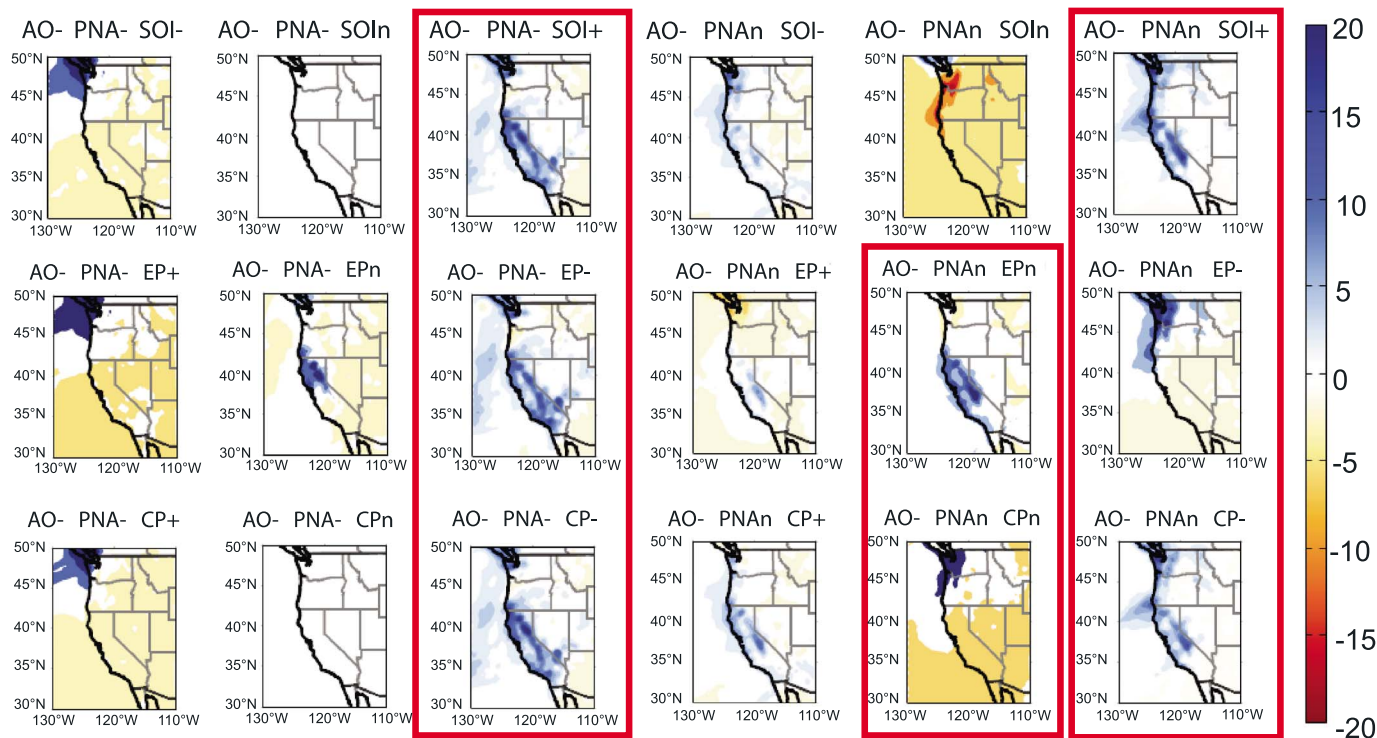


Figure 2. Maps of precipitation anomalies in the western U.S. during various climate mode combinations from 2001 to 2011. Maps were constructed utilizing NCEP North American Regional Reanalysis anomalous precipitation (mm) for days with extreme precipitation events (>100 mm at least one grid point in the selected domain) during specified combinations of the AO, PNA, and SOI climate indices. Shading shows regions more (blue) or less (red/yellow) likely to receive extreme precipitation during each combination. Red boxes highlight the specific combinations discussed in the text.

To construct the composite anomaly maps, we first calculated the 1979–2011 mean daily precipitation for each of the 365 (or 366) days. We then subtracted the long-term daily mean from all dates. Using the original data, we selected all days during 2001–2011 with precipitation events with at least one grid point in the western U.S. (110 – 130° W, 30 – 50° N) with >100 mm of precipitation. Using this subset, we then calculated and plotted the spatial pattern of composite (mean) daily anomalies during specified climate mode combinations (Figures 2 and S3a–S3e). Results of the composite analysis show that the combination of the negative AO, negative PNA, and positive SOI (La Niña) yielded the most widespread positive precipitation anomalies, essentially covering much of the state of California (Figure 2, left red box). This particular combination occurred during the largest precipitation event at our study site in December 2010, consistent with the tendency for extreme precipitation events in the southwest to be more intense during La Niña winters [Feldl and Roe, 2011]. This event was also characterized by an extremely negative $\delta^{18}\text{O}$ value (-16.89‰) at our site, suggesting that these extremely large, cold, and intense AR events during this climate mode combination may be especially well preserved in paleoclimate records. As the SOI, CP, and EP indices are closely related, similar results are generally seen when the CP and/or EP are negative. We also conducted a composite analysis of anomalous precipitation events during the AO–, PNA–, and SOI+ phase combination for the full NARR time period (1979 to 2011) and found similarly strong positive precipitation anomalies across much of the western U.S. (Figure 3a). Closer examination indicates that the 2001–2011 period was characterized by greater anomalous precipitation in Southern California and less in the Pacific Northwest (Figure 3b) compared with the full 1979–2011 period. This is highlighted by looking at the 2001–2011 minus 1979–2011 anomalies (Figure S5) which indicate that precipitation associated with this phase combination has increased in the southwestern U.S. and decreased in the northwestern U.S. relative to this phase combination's 1979–2011 climatology (Figures 3a–3c and S4). However, it is possible that this difference could partly be influenced by a single very large storm event, given the short period analyzed. Therefore, we are not able to make any robust conclusions about long-term trends from this analysis.

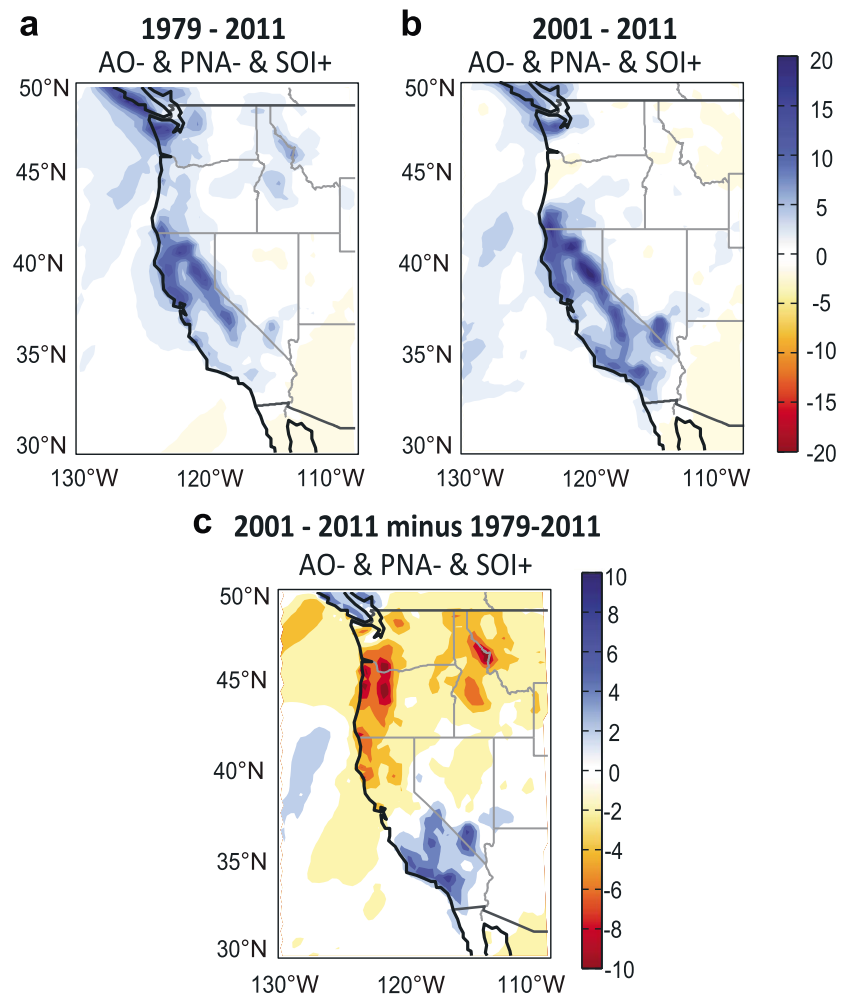


Figure 3. Climate mode composite maps show precipitation anomalies in the western U.S. based on North American Regional Reanalysis anomalous precipitation (mm) for days with extreme precipitation events (>100 mm at least one grid point in the selected domain) for the AO-, PNA-, and SOI+ phase combination for (a) 1979–2011, (b) 2001–2011, and (c) 2001–2011 minus 1979–2011.

While the type of ENSO event does not seem to significantly modify the precipitation anomaly pattern seen during the negative AO, negative PNA, and positive SOI combination, our results show that when the PNA is instead neutral, a prominent difference in the location of precipitation anomalies is seen between the two ENSO types. When the negative AO and neutral PNA occur together with a negative EP, anomalous precipitation is restricted to above $\sim 40^\circ\text{N}$, whereas the negative CP is characterized by anomalies extending below 40°N (Figure 2, right red box), consistent with a greater displacement of the Pacific jet stream during a Central Pacific type of ENSO event [Yu and Zou, 2013]. We also find that during the negative AO, neutral PNA, and neutral ENSO conditions, the Eastern Pacific neutral mode leads to anomalous precipitation delivered between ~ 35 and 42°N , whereas the Central Pacific neutral mode leads to less anomalous precipitation in this region. These results highlight that the ENSO type has an important influence over the regional distribution of anomalous precipitation delivered to the western U.S., especially when the AO is negative and the PNA is neutral (Figure 2, middle red box).

3. Conclusions

We investigated extreme precipitation events and their isotopic composition from the southwestern Sierra Nevada Mountains in California and the distribution of extreme precipitation across the western U.S. for varying coupled climate modes. We show that 90% of the extreme precipitation events at the CA study site

were ARs and occurred during the negative AO, with a weakened and split Aleutian Low and a strongly meridional jet stream. Furthermore, extreme precipitation at our site occurred more frequently during the positive SOI, though the relationship with SST-based ENSO indices is less clear. This suggests an atmospheric link between the tropical Walker circulation and AR frequency in the southwestern U.S., with large events being more likely when the Southern Oscillation is stronger. Stable isotope analysis of extreme precipitation reveals a large variability and indicates complex controls by a wide range of factors, including local temperature and precipitation amount (up to 25% of variance), moisture source region, and coupled climate modes, such as ENSO. A full assessment of the potential for stable isotopes to improve understanding of AR dynamics and as potential AR paleoproxies will likely require a more spatially and temporally dense isotopic study of AR precipitation and water vapor and the use of isotope-enabled climate models.

An analysis of NARR precipitation data from the western U.S. indicates that specific climate mode phase combinations particularly influence the spatial and temporal patterns of extreme precipitation anomalies. Composite maps demonstrate that extreme precipitation events in California are most likely when the negative AO, negative PNA, and positive SOI occur together. Additionally, the ENSO type, Eastern or Central Pacific, is shown to influence the landfall location of extreme precipitation anomalies across the western U.S., especially when the PNA is neutral. These results emphasize the importance of understanding the dynamic controls on extreme precipitation events in the western U.S. and highlight the use of various climate mode phase combinations to improve subseasonal and seasonal predictive capability for model projections. Furthermore, forced changes in atmospheric and coupled climate modes, such as ENSO and the AO, could influence the frequency, intensity, and landfalling position of AR events. For instance, Arctic amplification [Serreze and Barry, 2011] and projected sea ice decline [Deser et al., 2010] may lead to a more meridional jet stream and negative AO in the future, which would likely increase extreme precipitation across California. Knowledge of how tropical, midlatitude, and high-latitude climate modes influence extreme precipitation events in the western U.S. can provide critical information for short-term forecasting of extreme precipitation events. In addition, precipitation isotopes may be particularly useful for improving AR process understanding and may also be helpful as AR fingerprints in the paleoclimate record, but additional research is needed to fully assess this potential. These results will be potentially useful for improved long-term projections of extreme precipitation event frequency and location, but this will depend on improved model projections of the forced and unforced response of climate modes such as ENSO, the AO, and the PNA. Overall, improved projections of the likelihood and spatial pattern of extreme precipitation is critical for water planning and policy and flood risk analysis along the western coast of the U.S., especially in drought and flood prone California.

Acknowledgments

We thank Christopher Lehmann, Brenda Riney, and the National Atmospheric Deposition Program for providing precipitation samples and data used in this study; Dachun Zhang for water sample analysis; and Rick Behl, Jonathan Rutz, and two anonymous reviewers for useful comments on the paper. We also thank Martin Ralph for providing the dates of landfalling atmospheric river events utilized in this study. Composite maps were produced utilizing the plotting tools provided by the NOAA/ESRL Physical Sciences Division, Boulder, Colorado, on their website at <http://www.esrl.noaa.gov/psd/>. All precipitation and isotope data are available in the supporting information.

References

- Ault, A. P., C. R. Williams, A. B. White, P. J. Neiman, J. M. Creamean, C. J. Gaston, F. M. Ralph, and K. A. Prather (2011), Detection of Asian dust in California orographic precipitation, *J. Geophys. Res.*, *116*, D16205, doi:10.1029/2010JD015351.
- Barnes, E. A. (2013), Revisiting the evidence linking Arctic amplification to extreme weather in midlatitudes, *Geophys. Res. Lett.*, *40*, 4734–4739, doi:10.1002/grl.50880.
- Berkelhammer, M. B., and L. D. Stott (2008), Recent and dramatic changes in Pacific storm trajectories recorded in $\delta^{18}\text{O}$ from Bristlecone Pine tree ring cellulose, *Geochim. Geophys. Geosyst.*, *9*, Q04008, doi:10.1029/2007GC001803.
- Berkelhammer, M., L. Stott, K. Yoshimura, K. Johnson, and A. Sinha (2012), Synoptic and mesoscale controls on the isotopic composition of precipitation in the western United States, *Clim. Dyn.*, *38*, 433–454.
- Buening, N. H., L. Stott, K. Yoshimura, and M. Berkelhammer (2012), The cause of the seasonal variation in the oxygen isotopic composition of precipitation along the western U.S. coast, *J. Geophys. Res.*, *117*, D18114, doi:10.1029/2012JD018050.
- Bukovsky, M. S., and D. J. Karoly (2007), A brief evaluation of precipitation from the North American Regional Reanalysis, *J. Hydrometeorol.*, *8*, 837–846.
- Cayan, D. R., M. D. Dettinger, D. Pierce, T. Das, N. Knowles, F. M. Ralph, and E. Sumargo (2016), Natural variability, anthropogenic climate change, and impacts on water availability and flood extremes in the Western United States, in *Water Policy and Planning in a Variable and Changing Climate*, edited by K. A. Miller et al., pp. 17–42, CRC Press, Boca Raton, Fla.
- Cook, E. R., R. Seager, M. A. Cane, and D. W. Stahle (2007), North American drought: Reconstructions, causes, and consequences, *Earth Sci. Rev.*, *81*, 93–134.
- Craig, H. (1961), Isotopic variations in meteoric waters, *Science*, *133*, 1702–1703.
- Creamean, J. M., et al. (2013), Dust and biological aerosols from the Sahara and Asia influence precipitation in the western U.S., *Science*, *339*, 1572–1578.
- Dansgaard, W. (1964), Stable isotopes in precipitation, *Tellus*, *16*, 436–468.
- Deser, C., J. E. Walsh, and M. S. Timlin (2000), Arctic sea ice variability in the context of recent atmospheric circulation trends, *J. Clim.*, *13*, 617–633.
- Deser, C., R. Tomas, M. Alexander, and D. Lawrence (2010), The seasonal atmospheric response to projected Arctic sea ice loss in the late twenty-first century, *J. Clim.*, *23*, 333–351.
- Dettinger, M. (2004), Fifty-two years of “pineapple-express” storms across the West Coast of North America U.S. Geol. Surv., Scripps Institution of Oceanography for the California Energy Commission, PIER Project Rep.CEC-500-2005-004, 20.

- Dettinger, M. D. (2011), Climate change, Atmospheric Rivers, and floods in California—A multimodel analysis of storm frequency and magnitude changes, *J. Am. Water Resour. Assoc.*, *47*(3), 514–523, doi:10.1111/j.1752-1688.2011.00546.x.
- Feldl, N., and G. H. Roe (2011), Climate variability and the shape of daily precipitation: A case study of ENSO and the American West, *J. Clim.*, *24*, 2483–2499.
- Francis, J. A., and S. J. Vavrus (2012), Evidence linking Arctic amplification to extreme weather in mid-latitudes, *Geophys. Res. Lett.*, *39*, L06801, doi:10.1029/2012GL051000.
- Friedman, I., G. I. Smith, J. D. Gleason, A. Warden, and J. M. Harris (1992), Stable isotope composition of waters in southeastern California. 1: Modern precipitation, *J. Geophys. Res.*, *97*, 5795–5812, doi:10.1029/92JD00184.
- Gat, J. R. (1996), Oxygen and Hydrogen isotopes in the hydrologic cycle, *Annu. Rev. Earth Planet. Sci.*, *24*, 225–262.
- Guan, B., N. P. Molotch, D. E. Waliser, E. J. Fetzer, and P. J. Neiman (2013), The 2010/2011 snow season in California's Sierra Nevada: Role of Atmospheric Rivers and modes of large-scale variability, *Water Resour. Res.*, *49*, 6731–6743, doi:10.1002/wrcr.20537.
- Hagos, S. M., L. R. Leung, J.-H. Yoon, J. Lu, and Y. Gao (2016), A projection of changes in landfalling atmospheric river frequency and extreme precipitation over western North America from the Large Ensemble CESM simulations, *Geophys. Res. Lett.*, *43*, 1357–1363, doi:10.1002/2015GL067392.
- Kao, H., and J. Yu (2009), Contrasting eastern-Pacific and central-Pacific types of ENSO, *J. Clim.*, *22*, 615–632.
- Lavers, D. A., F. M. Ralph, D. E. Waliser, A. Gershunov, and M. D. Dettinger (2015), Climate change intensification of horizontal water vapor transport in CMIP5, *Geophys. Res. Lett.*, *42*, 5617–5625, doi:10.1002/2015GL064672.
- Liu, Z., K. Yoshimura, G. J. Bowen, and J. M. Welker (2014), Pacific–North American teleconnection controls on precipitation isotopes ($\delta^{18}\text{O}$) across the contiguous United States and adjacent regions: A GCM-based analysis, *J. Clim.*, *27*, 1046–1061.
- MacDonald, G. M., and R. A. Case (2005), Variations in the Pacific Decadal Oscillation over the past millennium, *Geophys. Res. Lett.*, *32*, L08703, doi:10.1029/2005GL022478.
- Mass, C., A. Skalenakis, and M. Warner (2011), Extreme precipitation over the West Coast of North America: Is there a trend?, *J. Hydrometeorol.*, *12*, 310–318.
- McCabe-Glynn, S., K. R. Johnson, C. Strong, M. Berkelhammer, A. Sinha, H. Cheng, and R. L. Edwards (2013), Variable North Pacific influence on drought in southwestern North America since AD 854, *Nat. Geosci.*, *6*, 617–621.
- Mesinger, F., G. DiMego, E. Kalnay, K. Mitchell, P. C. Shafran, W. Ebisuzaki, D. Jovic, J. Woollen, E. Rogers, and E. H. Berbery (2006), North American regional reanalysis, *Bull. Am. Meteorol. Soc.*, *87*, 343–360.
- Neiman, P. J., F. M. Ralph, G. A. Wick, J. D. Lundquist, and M. D. Dettinger (2008), Meteorological characteristics and overland precipitation impacts of Atmospheric Rivers affecting the West Coast of North America based on eight years of SSM/I satellite observations, *J. Hydrometeorol.*, *9*, 22–47.
- Overland, J. E., J. M. Adams, and N. A. Bond (1999), Decadal variability of the Aleutian Low and its relation to high-latitude circulation*, *J. Clim.*, *12*, 1542–1548.
- Payne, A. E., and G. Magnusdottir (2014), Dynamics of landfalling Atmospheric Rivers over the North Pacific in 30 years of MERRA reanalysis, *J. Clim.*, *27*, 7133–7150.
- Ralph, F., and M. Dettinger (2012), Historical and national perspectives on extreme West Coast precipitation associated with Atmospheric Rivers during December 2010, *Bull. Am. Meteorol. Soc.*, *93*, 783–790.
- Ralph, F. M., and M. D. Dettinger (2011), Storms, floods, and the science of Atmospheric Rivers, *Eos Trans. AGU*, *92*(32), 265–267, doi:10.1029/2011EO320001.
- Ralph, F. M., P. J. Neiman, and G. A. Wick (2004), Satellite and CALJET aircraft observations of Atmospheric Rivers over the eastern North Pacific Ocean during the winter of 1997/98, *Mon. Weather Rev.*, *132*, 1721–1745.
- Ralph, F. M., T. Coleman, P. J. Neiman, R. J. Zamora, and M. D. Dettinger (2013), Observed impacts of duration and seasonality of atmospheric-river landfalls on soil moisture and runoff in coastal Northern California, *J. Hydrometeorol.*, *14*, 443–459.
- Ralph, F., K. Prather, D. Cayan, J. Spackman, P. DeMott, M. Dettinger, C. Fairall, R. Leung, D. Rosenfeld, and S. Rutledge (2015), CalWater field studies designed to quantify the roles of Atmospheric Rivers and aerosols in modulating U.S. West Coast precipitation in a changing climate, *Bull. Am. Meteorol. Soc.*, doi:10.1175/BAMS-14-00043.1, in press.
- Ren, X., Y. Zhang, and Y. Xiang (2008), Connections between wintertime jet stream variability, oceanic surface heating, and transient eddy activity in the North Pacific, *J. Geophys. Res.*, *113*, D21119, doi:10.1029/2007JD009464.
- Rodionov, S., N. Bond, and J. Overland (2007), The Aleutian Low, storm tracks, and winter climate variability in the Bering Sea, *Deep Sea Res., Part II*, *54*, 2560–2577.
- Ryoo, J., D. E. Waliser, D. W. Waugh, S. Wong, E. J. Fetzer, and I. Fung (2015), Classification of atmospheric river events on the US West Coast using a trajectory model, *J. Geophys. Res. Atmos.*, *120*, 3007–3028.
- Screen, J. A., and I. Simmonds (2014), Amplified mid-latitude planetary waves favour particular regional weather extremes, *Nat. Clim. Change*, *4*, 704–709, doi:10.1038/nclimate2271.
- Sellers, S., P. Nguyen, W. Chu, X. Gao, K. Hsu, and S. Sorooshian (2013), Computational Earth science: Big data transformed into insight, *Eos Trans. AGU*, *94*, 277–278, doi:10.1002/2013EO320001.
- Serreze, M. C., and R. G. Barry (2011), Processes and impacts of Arctic amplification: A research synthesis, *Global Planet. Change*, *77*, 85–96.
- Stone, R. C., G. L. Hammer, and T. Marcussen (1996), Prediction of global rainfall probabilities using phases of the Southern Oscillation Index, *Nature*, *384*, 252–255, doi:10.1038/384252a0.
- Strong, C., and G. Magnusdottir (2008), Tropospheric Rossby wave breaking and the NAO/NAM, *J. Atmos. Sci.*, *65*, 2861–2876.
- Thompson, D. W., and J. M. Wallace (2000), Annular modes in the extratropical circulation. Part I: Month-to-month variability*, *J. Clim.*, *13*, 1000–1016.
- Trenberth, K. E. (1999), Conceptual framework for changes of extremes of the hydrological cycle with climate change, *Clim. Change*, *42*, 327–339.
- Vachon, R., J. Welker, J. White, and B. Vaughn (2010), Monthly precipitation isoscapes ($\delta^{18}\text{O}$) of the United States: Connections with surface temperatures, moisture source conditions, and air mass trajectories, *J. Geophys. Res.*, *115*, D21126, doi:10.1029/2010JD014105.
- Welker, J. M. (2012), ENSO effects on $\delta^{18}\text{O}$, $\delta^2\text{H}$ and d-excess values in precipitation across the US using a high-density, long-term network (USNIP), *Rapid Commun. Mass Spectrom.*, *26*, 1893–1898.
- Wick, G. A., P. J. Neiman, and F. M. Ralph (2013), Description and validation of an automated objective technique for identification and characterization of the integrated water vapor signature of Atmospheric Rivers, *IEEE Trans. Geosci. Remote Sens.*, *51*, 2166–2176.
- Wise, E. K., and M. P. Dannenberg (2014), Persistence of pressure patterns over North America and the North Pacific since AD 1500, *Nat. Commun.*, *5*, 4192, doi:10.1038/ncomms5912.

- Yoshimura, K., M. Kanamitsu, D. Noone, and T. Oki (2008), Historical isotope simulation using reanalysis atmospheric data, *J. Geophys. Res.*, *113*, D19108, doi:10.1029/2008JD010074.
- Yoshimura, K., M. Kanamitsu, and M. Dettinger (2010), Regional downscaling for stable water isotopes: A case study of an atmospheric river event, *J. Geophys. Res.*, *115*, D18114, doi:10.1029/2010JD014032.
- Yu, J., and H. Kao (2007), Decadal changes of ENSO persistence barrier in SST and ocean heat content indices: 1958–2001, *J. Geophys. Res.*, *112*, D13106, doi:10.1029/2006JD007654.
- Yu, J., and S. T. Kim (2010), Identification of central-Pacific and eastern-Pacific types of ENSO in CMIP3 models, *Geophys. Res. Lett.*, *37*, L15705, doi:10.1029/2010GL044082.
- Yu, J., and Y. Zou (2013), The enhanced drying effect of Central-Pacific El Niño on US winter, *Environ. Res. Lett.*, *8*, 014019.
- Yu, J., Y. Zou, S. T. Kim, and T. Lee (2012), The changing impact of El Niño on US winter temperatures, *Geophys. Res. Lett.*, *39*, L15702, doi:10.1029/2012GL052483.
- Zhu, Y., and R. E. Newell (1998), A proposed algorithm for moisture fluxes from Atmospheric Rivers, *Mon. Weather Rev.*, *126*, 725–735.
- Zou, Y., J. Yu, T. Lee, M. Lu, and S. T. Kim (2014), CMIP5 model simulations of the impacts of the two types of El Niño on the US winter temperature, *J. Geophys. Res. Atmos.*, *119*, 3076–3092, doi:10.1002/2013JD021064.